Development of Helicopter Flight Path Models

Alfred Fermelia

Donald A. Gyorog
Missouri University of Science and Technology

V. J. Flanigan
Missouri University of Science and Technology

Development of Helicopter Flight Path Models

A. FERMELIA
Hughes Aircraft Co.
Buckley Air National Guard Base
Aurora, CO

D.A. GYOROG
Rodman Laboratory
Rock Island Arsenal
Rock Island, IL

V.J. FLANIGAN
University of Missouri–Rolla
Rolla, MO

Manuscript received June 2, 1976.

This work was sponsored in part by the National Science Foundation by the U.S. Army Armaments Command, and by the University of Missouri–Rolla.

Introduction

The objective of this paper is to present general techniques for simulating helicopter flight trajectory response. During flight the pilot manipulates the controls either to trim the helicopter for steady flight by balancing the external forces and moments or to produce a desired maneuver by controlling the unbalance of these forces and moments. Discussions of the physical phenomena involved with the aerodynamics of the rotors and fuselage are given in [1] through [3].

The simulated control function will be composed forward-aft cyclic, lateral cyclic, pedal, and collective. This control will be represented by the vector

$$\mathbf{u} = \begin{cases} u_1 \triangleq \text{collective} \\ u_2 \triangleq \text{lateral cyclic} \\ u_3 \triangleq \text{longitudinal cyclic} \\ u_4 \triangleq \text{pedal} \end{cases} \tag{1}$$

The purpose of the pilot control input is to create necessary aerodynamic forces and moments to control helicopter motion and attitude which is measured by the center of gravity velocity and the angular orientation (yaw, pitch, and roll) and velocity of the fuselage. This output state will be denoted by the vector

$$\mathbf{x} = \begin{cases} \left.\begin{matrix} u \\ v \\ w \end{matrix}\right\} \text{velocity of the center of gravity} \\ \left.\begin{matrix} p \\ q \\ r \end{matrix}\right\} \text{angular velocity of the fuselage} \\ \left.\begin{matrix} \psi \\ \theta \\ \phi \end{matrix}\right\} \text{angular orientation of the fuselage} \\ \Omega \} \text{ rotor speed} \end{cases} \tag{2}$$

To provide closed-loop action for the simulation, the control model must interpret the necessary control **u** as a result of any deviation in **x** from the desired state. Fig. 1 illustrates the overall concept of the flight path simulation in block diagram form.

The blocks numbered 1 through 5 are associated with the helicopter dynamics model. Discussion of the model applied to this study is given in [4], [11], and [13]. The linearized version of the dynamics model [13] provides the basic representation of the helicopter response for the solution of the control problem. In the present study only block 8 will be considered. Hence the pilot control action, block 9 of Fig. 1, has been assumed to be a unit gain which implies that the control goal is instantaneously predicted.

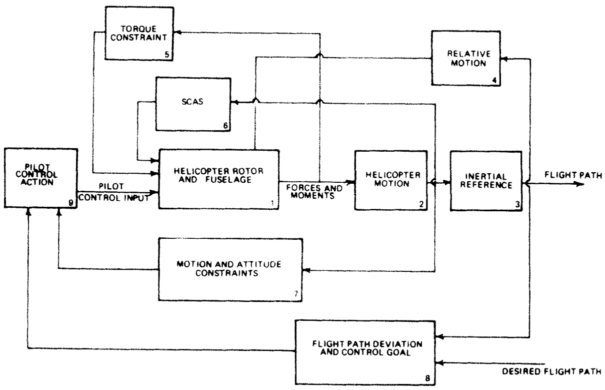

Fig. 1. Helicopter flight path model.

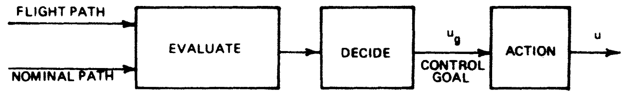

Fig. 2. Pilot model function.

Fig. 3. Control problem.

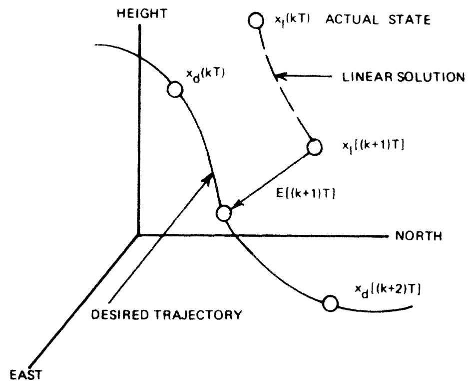

Nomenclature

$E \triangleq$ Error function.
$J \triangleq$ Objective function.
$\mathbf{u} \triangleq$ Nominal control vector.
$\mathbf{u}_g \triangleq$ Control goal.
$\delta \mathbf{u} \triangleq$ Perturbed control.
$W_E \triangleq$ Symmetric positive definite state weighting function.
$W_u \triangleq$ Symmetric positive definite control weighting function.
$\mathbf{x}_d \triangleq$ Desired state vector.
$\mathbf{x}_l \triangleq$ Linearized state vector.
$\delta_\mathbf{x} \triangleq$ Perturbed state vector.
$\phi \triangleq$ Stability matrix.
$\theta \triangleq$ Control matrix.

Deterministic Control Model

Two basic approaches to developing a mathematical representation of the human operator's data sampling, error quantization, and control goal decision roles can be defined. These two approaches are significantly different in their characterization of the operator. One method involves the qualitative and psychological aspects of the pilot. Functions such as sensing of the aircraft state and various instruments, the categorizing of these measurements as acceptable or nonacceptable, the human prediction and memory capability, and the human ability to adapt his response to the given situation would be included in this type of model. Probably one of the better illustrations of this approach is given by Benjamin [6]. His study involved the relatively less complicated case of single input-output tracking, whereas the helicopter pilot has four control inputs at his disposal with the desirability of controlling at least 10 output variables. Adding this dynamic model complexity to an operator model such as Benjamin's which is elaborate from the standpoint of the logic structure was not feasible due to computer limitations.

The second approach can be entitled a quasi-pilot engineering model which describes the overall performance of the pilot without close regard to psychological function of the human operator. Some authors [7] have referred in general to these two approaches in a descriptive way as microscopic and macroscopic modeling of the pilot, respectively. From the results of the many previous investigations concerned with the modeling of a human operator in various tasks, it became apparent that the engineering model approach was the most feasible based on the current simulation state of the art.

The essential functions of a pilot model are to evaluate the system error, predict the necessary control input goal, and perform the control input manipulation, as illustrated in Fig. 2. Thus in Fig. 1 the pilot control model provides the feedback required for the closed-loop simulation of the helicopter flight path in conjunction with the helicopter dynamics model. Since the development of the pilot logic for a general maneuver was impractical, the desired or nominal trajectory for the helicopter state is prescribed [5]. Comparison of this nominal with the actual state produces the error from which the control goal can be resolved.

From the desired trajectory, the state $\mathbf{x}_d(t)$ is known at discrete time intervals $0, T, \cdots, kT, \cdots$, etc., as depicted in Fig. 3. In addition, from the trimmed flight conditions, the initial state $\mathbf{x}(0)$ and the control vector $\mathbf{u}(0)$ are known. It is presumed that the starting point of the trajectory will be a steady or trimmed flight condition. With these quantities given as initial data the helicopter dynamics portion of the simulation will yield the new state at $t = T$, i.e., $x(T)$. At the time T a new selection of control is necessary for the next interval T to $2T$. The control vector is constant for the length of the discrete sampling time and is only changed by some amount $\delta u(kT)$ at the next sampling instant. With the new control the dynamics model again yields the subsequent state of the helicopter. This respective process continues for the desired time of the prescribed nominal path. The question to be answered is, what control goal or change of control is required at each of the sampling times?

For small perturbations the nonlinear helicopter dynamics can be approximated by the linear state equation (13)

$$\delta\dot{\mathbf{x}}(t) = A\delta\mathbf{x}(t) + B\,\delta u(t) \tag{3}$$

where the system and control time-invariant matrices A and B are evaluated at the particular state from which the control change is to be calculated. The solution of (3) for the time interval kT to $(k+1)T$ is known to be [8]-[10]

$$\delta x_i\{(k+1)T\} = \phi(T)\,\delta\mathbf{x}(kT) + \theta(T)\,\delta\mathbf{u}(kT) \tag{4}$$

where ϕ is a (10×10) stability matrix and θ is a (10×4) control matrix.

Since the desired state vector is given at the discrete time increments $\mathbf{x}_d\,(kT)$, it is proposed that the necessary control goal $u_g(kT)$ follow the desired path be calculated with the simplified linear model. The selected goal should minimize the deviation between the nominal and linear helicopter states. Hence a cost function J which provides the basis for selecting the best control vector should include both of these considerations. For convenience, a quadratic form is defined

$$J = E^{\mathrm{T}}\{(k+1)T\}\,W_E\{(k+1)T\}\,E\{(k+1)T\}. \tag{5}$$

The function J is to be minimized by the proper selection of $\mathbf{u}(kT)$ where W_e is a time-varying matrix for the predicted state error at time $(k+1)T$. Note that the predicted error at the time $(k+1)T$ is

$$E\{(k+1)T\} = \mathbf{x}_d\{(k+1)T\} - \mathbf{x}_l\{(k+1)T\} \tag{6}$$

but from (4) with $\mathbf{x}_l(kT)$ set equal to the actual state $\mathbf{x}(kT)$, the cost functional is

$$\begin{aligned} J = {} & \mathbf{x}_d^{\mathrm{T}}\{(k+1)T\}\,W_E\{(k+1)T\}\,\mathbf{x}_d\{(k+1)T\} \\ & - 2\mathbf{x}_d^{\mathrm{T}}\{(k+1)T\}\,W_E\{(k+1)T\}\,\mathbf{x}_d\{(k+1)T\} \\ & - 2\mathbf{x}_d^{\mathrm{T}}\{(k+1)T\}\,W_E\{(k+1)T\}\{\phi(T)\,\delta\mathbf{x}\{(k-1)T\} \\ & + \theta(T)\,\delta u\{(k-1)T\} + \{\phi(T)\,\delta\mathbf{x}\{(k-1)T\} \\ & + \theta(T)\,\delta\mathbf{u}\{(k-1)T\}\}^{\mathrm{T}}\,W_E\{(k+1)T\} \\ & \cdot \{\phi(T)\,\delta\mathbf{x}\{(k-1)T\} + \theta(T)\delta\mathbf{u}\{(k-1)T\}. \end{aligned} \tag{7}$$

Therefore in order to minimize the cost functional the control $\mathbf{u}_g(kT)$ is given by

$$\mathbf{u}_g(kT) = \mathbf{u}\{(k-1)T\} + \delta\mathbf{u}\{(k-1)T\} \tag{8}$$

where

$$\begin{aligned} \delta\mathbf{u}^{\mathrm{T}}\{(k-1)T\} = {} & \{\mathbf{x}_d^{\mathrm{T}}\{(k+1)T\} - (x(kT) \\ & + \phi(T)\,\delta\mathbf{x}\{(k-1)T\})^{\mathrm{T}}\} \\ & \cdot W_E\{(k+1)T\}\,\theta(T)\{\theta^{\mathrm{T}}(T) \\ & \cdot W_E\{(k+1)T\}\,\theta(T)\}^{-1}. \end{aligned} \tag{9}$$

Application of the control law given by (8) and (9) to certain desired flight paths results in a maximum/minimum control. Therefore in order to avoid this condition alternate cost functions can be considered.

If the computed control is not feasible,[1] then an obvious solution is to minimize an objective function which weighs the control, i.e., consider

$$\begin{aligned} J = {} & E^{\mathrm{T}}\{(k+1)T\}\,W_E\{(k+1)T\}\,E\{(k+1)T\} \\ & + \delta\mathbf{u}^{\mathrm{T}}\{(k-1)\}\,W_u\{(k-1)T\}\,\delta\mathbf{u}\{(k-1)T\}. \end{aligned} \tag{10}$$

The control that minimizes (10) is given by

$$\begin{aligned} \delta\mathbf{u}^{\mathrm{T}}\{(k-1)T\} = {} & \{\mathbf{x}_d^{\mathrm{T}}\{(k+1)T\} - (\mathbf{x}^{\mathrm{T}}(kT) \\ & + \delta\mathbf{x}^{\mathrm{T}}\{(k-1)T\}\,\phi^{\mathrm{T}}(T))\} \\ & \cdot W_E\{(k+1)T\}\,\theta(T)\{\theta^{\mathrm{T}}(T) \\ & \cdot W_E\{(k+1)T\}\,\theta(T) \\ & + W_u\{(k-1)T\}^{-1}. \end{aligned} \tag{11}$$

Generation of this control for certain desired flight paths resulted in a control vector $\mathbf{u}$ which was not feasible. Clearly this control could satisfy the control constraints provided the time-varying weighting matrix W_u is chosen correctly. Therein lies the problem, i.e., how does one choose the weighting matrix W_e as a function of time? Attempts were made to select W_u to limit excursion of control to no avail.

In order to motivate the algorithm which does produce a control that satisfies all control limit constraints, consider (11). Note the effect of the control weighting function is to add to the penalty associated with the state error, i.e., the last term in brackets of (11). Therefore with the control given by (9), this equation can be written as

$$\delta u^{\mathrm{T}}\{(k-1)T\} = \tilde{x}\{(k+1)T\}\{\theta^{\mathrm{T}}(T)\,W_E\{(k+1)T\}\theta(T)\}^{-1} \tag{12}$$

where

$$\begin{aligned} \tilde{x}\{(k+1)T\} \triangleq {} & \{\mathbf{x}_d\{(k+1)T\} - (\mathbf{x}(kT) \\ & + \phi(T)\,\delta\mathbf{x}\{(k-1)T\})^{\mathrm{T}}\} \\ & \cdot W_E\{(k+1)T\}\,\theta(T). \end{aligned}$$

[1] Control constraints are given in Table I.

TABLE I
Control Constraints

CONTROL	UPPER LIMIT (RADIANS)	LOWER LIMIT (RADIANS)
LATERAL CYCLIC	0.122	-0.189
LONGITUDINAL CYCLIC	0.230	-0.230
COLLECTIVE PITCH	0.353	0.140
TAIL ROTOR PITCH	0.401	-0.122

Comparing (11) and (12) indicates that if

$$\{\theta^T(T)\, W_E\{(k+1)T\}\, \theta(T) + W_u\{(k-1)T\}^{-1}$$
$$= \{\theta^T(T)\, W_E\{(k+1)T\}\, \theta(T)\}^{-1}$$

the two equations are identical and for simplicity

$$\{\theta^T(T)\, W_{EU}\{(k+1)T\}\, \theta(T)\}^{-1}$$
$$= \{\theta^T(T)\, W_E\{(k+1)T\}\, \theta(T)\}^{-1}. \tag{13}$$

Now assume that the control law generated using (9) is not feasible. The solution for the kT time is given by

$$\delta \mathbf{u}_j^T(kT) = \tilde{\mathbf{x}}^T\{(k+2)T\}\{\theta^T(T)\, W_E\{(k+2)T\}\, \theta(T)\}^{-1}. \tag{14}$$

Solving for $\tilde{\mathbf{x}}\{(k+2)T\}$ yields

$$\tilde{\mathbf{x}}_j^T\{(k+2)T\} = \delta \mathbf{u}^T(kT)\{\theta^T(T)\, W_E\{(k+2)T\}\, \theta(T)\}. \tag{15}$$

Since the control is not acceptable, i.e., it is too large or too small, an iteration that will guarantee feasibility can be defined. The first jth iteration is given by (14), the $(j+1)$th iteration yields the control

$$\delta \mathbf{u}_{j+1}^T(kT) = \tilde{\mathbf{x}}^T\{(k+2)T\}\{\theta^T(T)\, W_{EU}\theta(T)\}^{-1}. \tag{16}$$

Therefore it follows that

$$\tilde{\mathbf{x}}^T\{(k+2)T\} = \delta \mathbf{u}_{j+1}^T(kT)\{\theta^T(T)\, W_{EU}\theta(T)\}. \tag{17}$$

In essence the objective function in the jth iteration is (5), whereas the $(j+1)$th iteration utilizes the cost function given in (10). However the necessity to select both a weighting matrix for state and one for the control no longer exists.

In order to demonstrate the feasibility of the control consider

$$\delta \mathbf{u}_j^T(kT)\, \delta \mathbf{u}_j(kT) = \tilde{\mathbf{x}}^T\{(k+2)T\}[\{\theta^T(T)$$
$$\cdot W_E\{(k+2)T\}\, \theta(T)\}^{-1}$$
$$\cdot \{\theta^T(T)\, W_E\{(k+1)T\}\, \theta(T)\}^{-1}]$$
$$\cdot \tilde{\mathbf{x}}\{(k+2)T\}. \tag{18}$$

Substituting (17) into (18) yields

$$\delta \mathbf{u}_j^T(kT)\, \delta \mathbf{u}_d(kT) = \delta \mathbf{u}_{j+1}^T(kT)\, \{\theta^T(T)\, W_{EU}\theta(T)\}$$
$$\cdot \{\theta^T(T)\, W_E\{(k+2)T\}\, \theta(T)\}^{-1}$$
$$\cdot \{\theta^T(T)\, W_E\{(k+2)T\}\, \theta(T)\}^{-1}$$
$$\cdot \{\theta^T(T)\, W_{EU}\theta(T)\}^T\, \delta \mathbf{u}_{j+1}(kT). \tag{19}$$

Then subtracting $\delta \mathbf{u}_j^T\, \delta \mathbf{u}_j$ from $\delta \mathbf{u}_{j+1}$ yields

$$\delta \mathbf{u}_{j+1}^T \delta \mathbf{u}_{j+1} - \delta \mathbf{u}_j^T \delta \mathbf{u}_j = \delta \mathbf{u}_{j+1}^T\, \{I - \theta^T W_{EU}\theta\{(\theta^T W_E\theta)^{-1}$$
$$\cdot (\theta^T W_E\theta)^{-1}\}\theta^T W_{EU}\theta\}\, \delta \mathbf{u}_{j+1} \tag{20}$$

where the time parameters have been omitted. Now in order that the $(j+1)$th iteration be less than the jth iteration, the term in brackets must be less than a preselected negative definite matrix P, i.e., where

$$I - RMR \leqslant P \tag{21}$$

with $R \triangleq \theta^T W_{EU}\theta$ and $M \triangleq (\theta^T W_E\theta)^{-1}\, (\theta^T W_E\theta)^{-T}$. Note the matrix M is a known constant; hence solving (21) for R will insure a feasible control.

Results and Conclusions

In order to demonstrate the application of the described techniques to helicopter motion, four flight paths were considered. These consisted of level flight, climb, dive, and a turn/climb. In order to compare nonlinear versus linear models, inertial position and angular velocities of the helicopter were plotted as a function of time (Figs. 4 through 33).

Very little distinction could be made between the nonlinear and linear directional motion for the level, climb, and dive configuration; i.e., north-south, east-west type motion of predicted corresponds with the nominal—see [11].

Comparison of Figs. 5, 12, 19, and 27 indicates that the predicted roll matches the desired state within ±0.4 rad. Although roll was not matched as well in the climb orientation, it nevertheless matches the shape of the desired

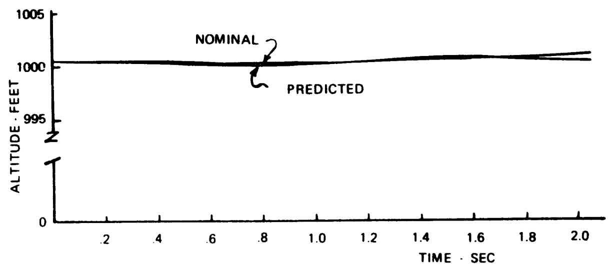

Fig. 4. Inertial position for level flight.

Fig. 5. Level flight roll versus time.

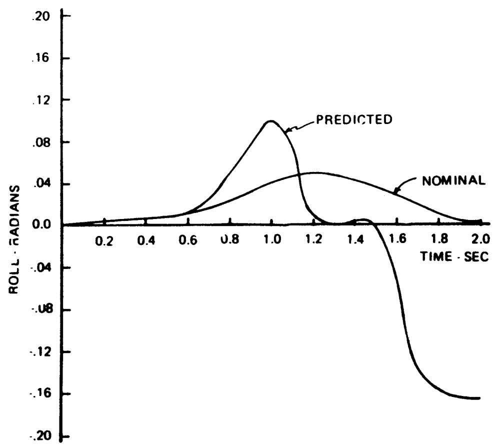

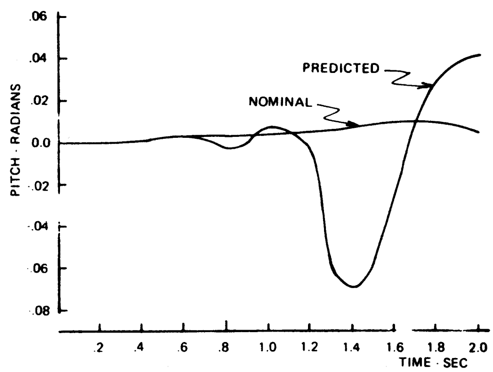

Fig. 6. Level flight pitch versus time.

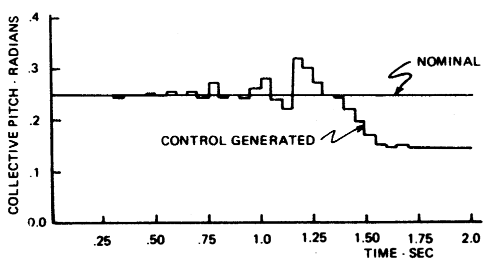

Fig. 7. Level flight collective pitch.

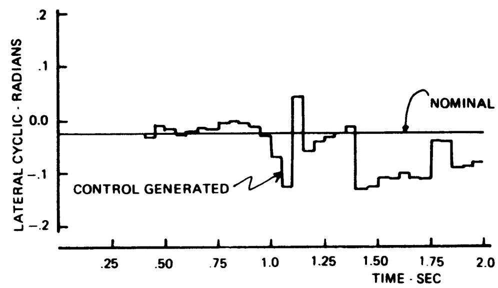

Fig. 8. Level flight lateral cyclic.

Fig. 9. Level flight longitudinal cyclic.

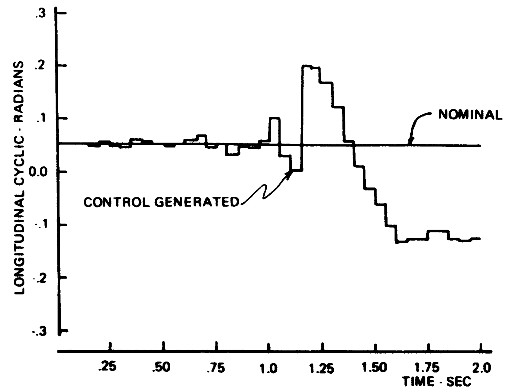

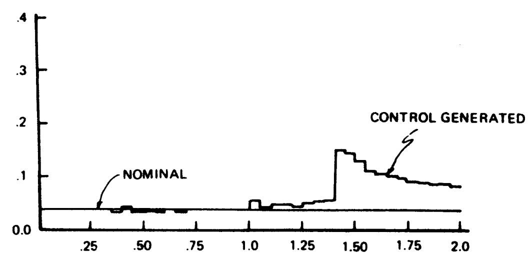

Fig. 10. Level flight tail rotor pitch.

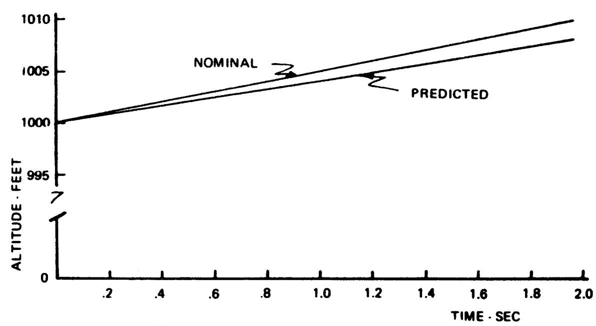

Fig. 11. Inertial position for climb configuration.

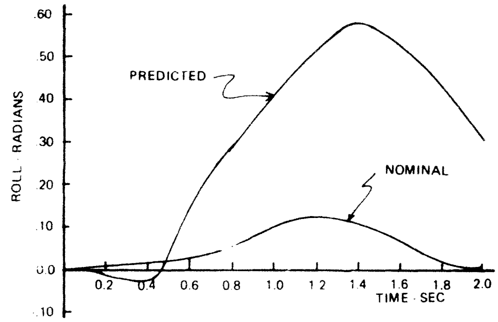

Fig. 12. Climb configuration roll versus time.

Fig. 13. Climb configuration pitch versus time.

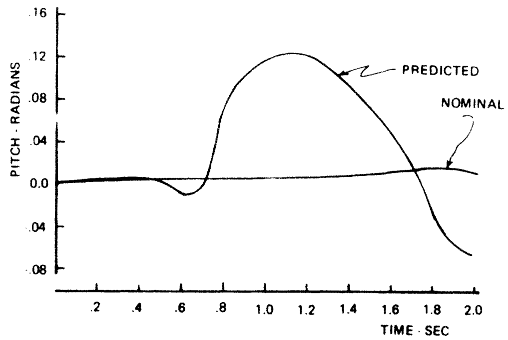

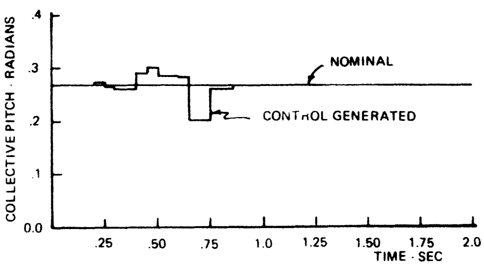

Fig. 14. Climb configuration collective pitch.

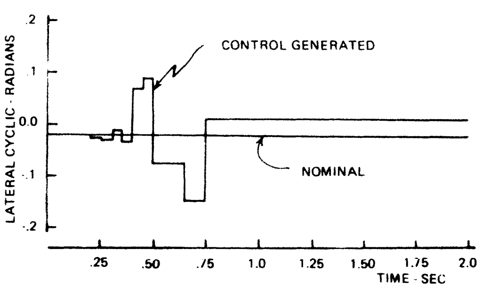

Fig. 15. Climb configuration lateral cyclic.

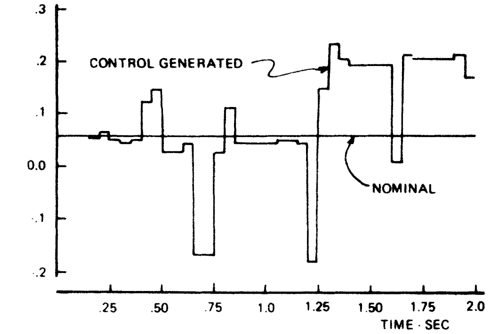

Fig. 16. Climb configuration longitudinal cyclic.

Fig. 17. Climb configuration tail rotor pitch.

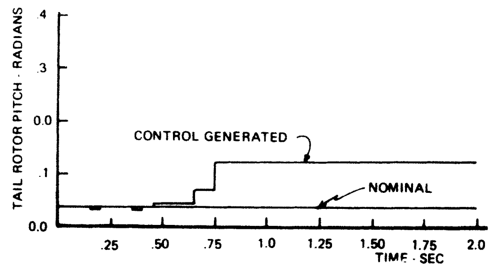

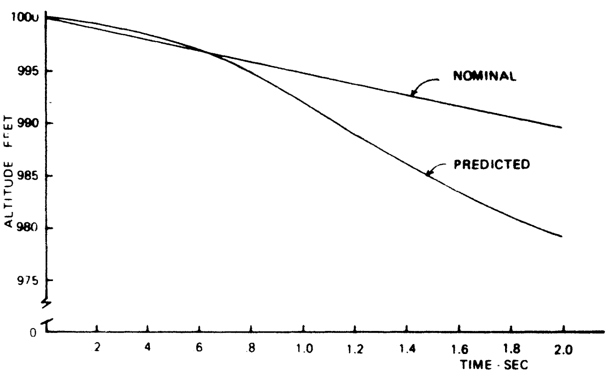

Fig. 18. Inertial position for dive configuration.

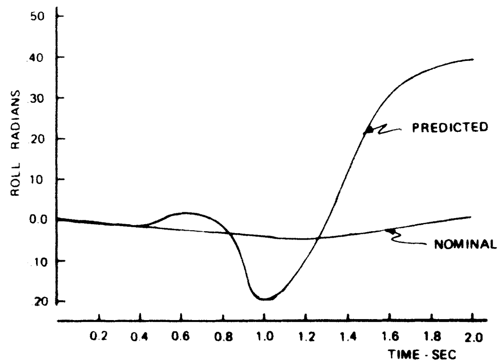

Fig. 19. Dive configuration roll versus time.

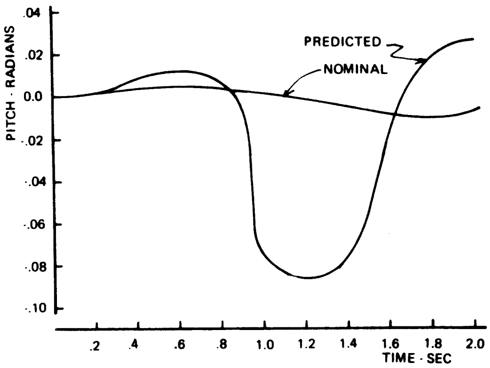

Fig. 20. Dive configuration pitch versus time.

Fig. 21. Dive configuration collective pitch.

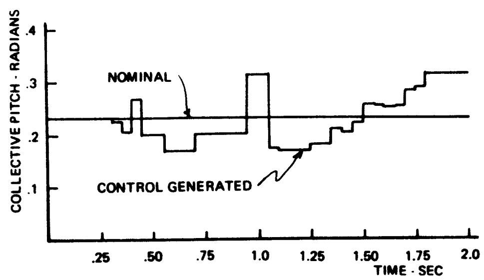

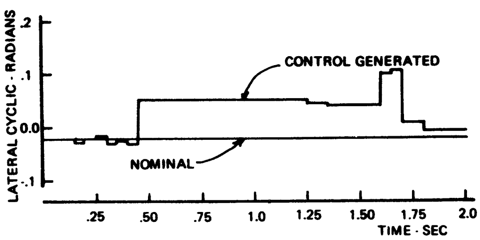

Fig. 22. Dive configuration lateral cyclic.

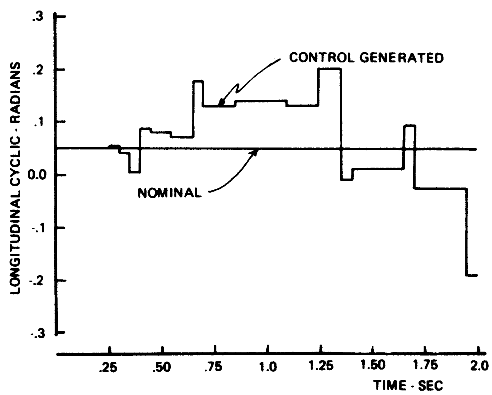

Fig. 23. Dive configuration longitudinal cyclic.

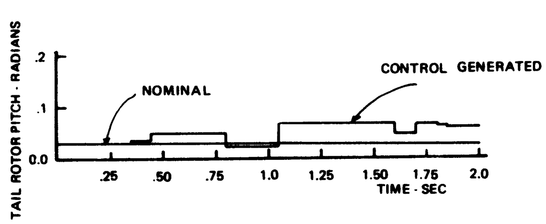

Fig. 24. Dive configuration tail rotor pitch.

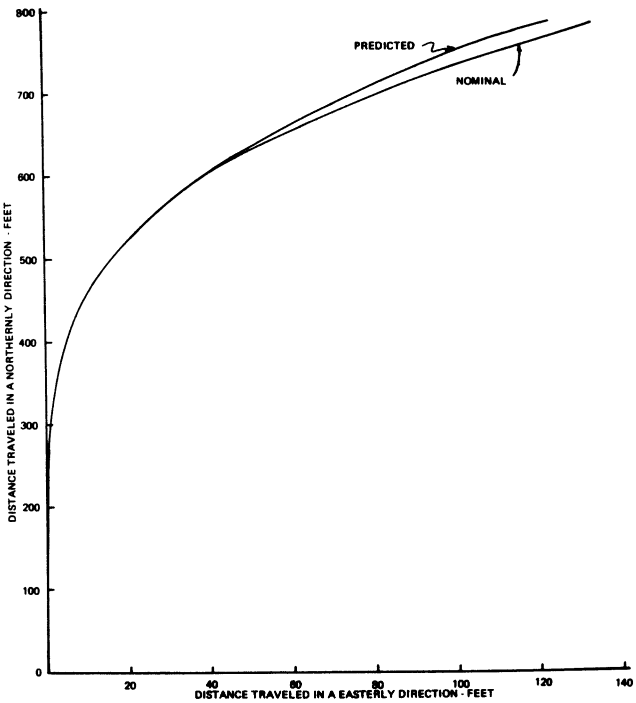

Fig. 25. Inertial position for turn configuration.

Fig. 26. Turn configuration altitude versus time.

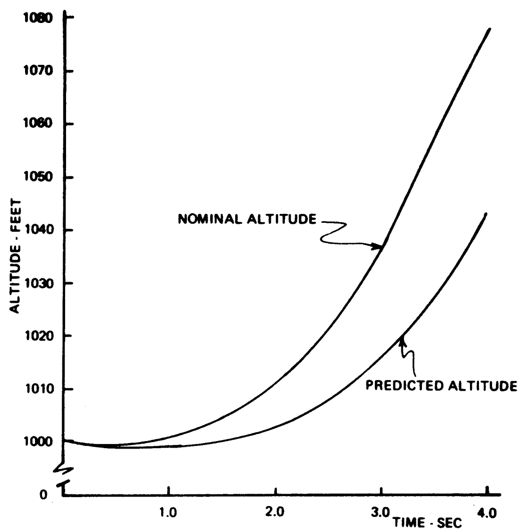

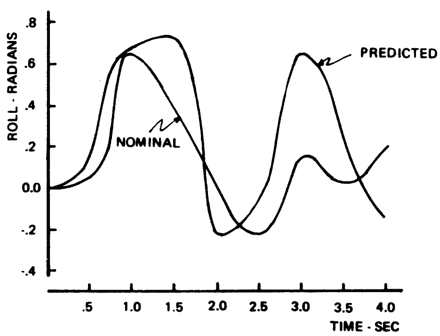

Fig. 27. Turn configuration roll versus time.

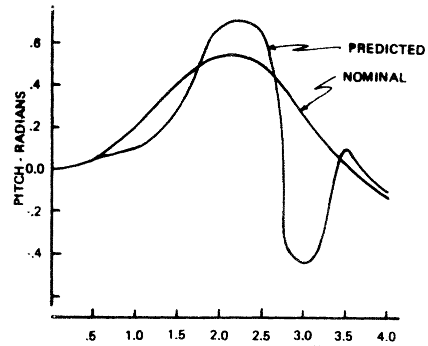

Fig. 28. Turn configuration pitch versus time.

Fig. 29. Turn configuration yaw versus time.

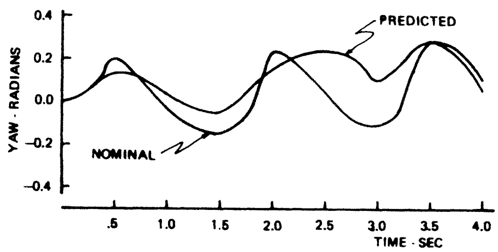

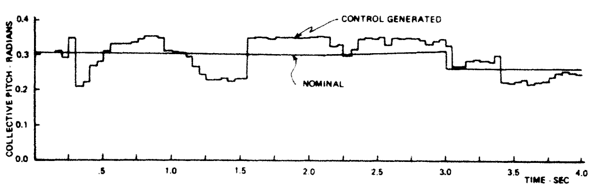

Fig. 30. Turn configuration collective pitch.

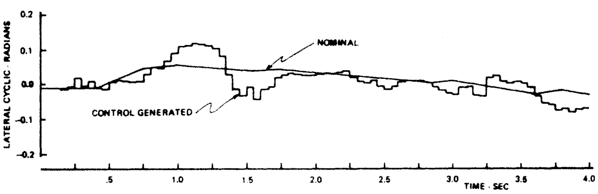

Fig. 31. Turn configuration lateral cyclic.

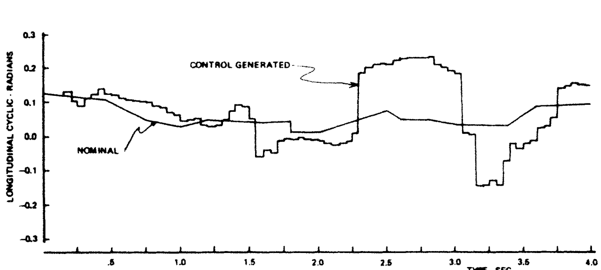

Fig. 32. Turn configuration longitudinal cyclic.

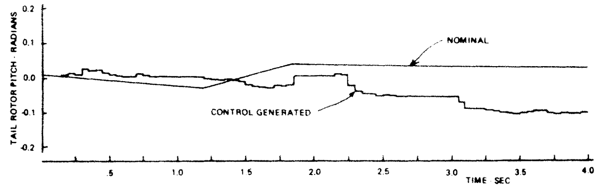

Fig. 33. Turn configuration tail rotor pitch.

state better than that of the level flight or dive. Note that in the turn flight path, the shape of the predicted roll closely follows the desired trajectory. Examination of the figures also reveals that the linear model attempts to follow the trend of the desired for those flight paths which give rise to maximum motion; i.e., examine the roll histograms. The oscillatory nature of Fig. 19 may be explained by noting that the system to be controlled is of the tenth order. Note that the frequency content of the desired roll is quite low; hence the control of the roll parameter is delegated a lower priority than the control responsible for controlling the forward velocity. This is illustrated by Figs. 21 through 24 which give the control histograms for the dive trajectory.

As might be expected, results of the climb flight path are mirrored in the dive trajectory. This is very apparent when comparing the time traces of pitch for both cases. The stability of the level flight might be questioned after examination of the pitch channel for that particular configuration. However, noting that the amplitude at the end of 2 s is less than that obtained at 1.4 s gives an indication that the trajectory is stable. Credence to this conjecture is given by examination of the pitch channel for the turn/climb, i.e., the turn/climb consists of a level flight for the first 2 s.

Having examined the characteristics of roll and pitch, expectations are that the yaw channel would exhibit the same type of performance. Reference [11] shows that this is indeed true.

The turn/climb configuration exhibited very good agreement between the nominal and predicted trajectories. Note that during the turn the vehicle simultaneously undergoes a climb, i.e., a constant rate of turn is not experienced. In order to obtain the turn/climb trajectory, control positions were taken from actual flight test data. These control positions were input as nominal values into the nonlinear model which resulted in the turn/climb trajectory. This trajectory was then input as the desired flight path which the linear model attempted to fit. Figs. 25-33 illustrate the results obtained.

It is interesting to note that in all angular velocity channels the response in the linear model appears to lag behind that of the desired flight path. Also, in every case considered the magnitude of the response is much larger than that of the nominal. This is best illustrated by Fig. 12. Cause of these anomalies can be explained by the linear model chosen to represent the nonlinear helicopter. In selecting a suitable model to approximate the helicopter two linear configurations were initially considered. The models considered were

$$\delta x_i\{(k+1)T\} = \phi(T)\,\delta x(kT) + \theta(T)\,\delta u(kT) \tag{22}$$

and

$$\delta x_i\{(k+1)T\} = \phi(T)\,\delta x(kT) + \psi(T, T-1)\,\delta x\{(k-1)\} + \theta(T)\,\delta u(kT) + \Gamma\{T, T-1\} \cdot \delta u\{(k-1)T\}. \tag{23}$$

Equation (22) was chosen for the following reasons: 1) references [11] and [13] indicate that it could indeed approximate the nonlinear model, 2) a model similar to (22) was used in [12], and 3) simplicity of (22) as compared to the complexity of (23).

The anomalies mentioned above can be explained by the omission in (22) of information contained in the coefficient matrices ψ and Γ of (23). By neglecting ψ, information regarding the frequency content of the system will be lost. Similarly omission of Γ may result in generation of a control law which exceeds the bounds of a feasible control.

In conclusion, this study demonstrated that control techniques can be applied to a helicopter flight simulation which allows the vehicle to follow a predetermined nominal flight path. However, due to approximations in the linear model, a technique had to be developed whereby a feasible control law could be obtained. In order to achieve this, an algorithm was developed to determine a weighting matrix as a function of time. This technique can be implemented on other systems with a similar effect.

References

[1] A. Gessow, and G. Meyers, Jr., *Aerodynamics of the Helicopter.* New York: MacMillan, 1952.

[2] A. Nikolsky, *Helicopter Analysis.* New York: Wiley, 1951.

[3] D. Gyorog, "Helicopter rotor analysis," U.S. Army Weapons Command Rep., Nov. 1970.

[4] A. Fermelia, J. Matson, and D. Gyorog, "Helicopter flight path simulation, pt. I: Helicopter dynamics (ECOM) model," U.S. Army Weapons Command Rep., Oct. 1971.

[5] D. Gyorog, and A. Fermelia, "Helicopter flight path simulation, pt. II: Pilot model preliminary analysis," U.S. Army Weapons Command Rep., Oct. 1971.

[6] P. Benjamin, "A hierarchial model of a helicopter pilot," *Human Factors,* vol. R, pp. 361-374, Aug. 1970.

[7] A.L. Burgett, "A study of human operator performance using regression analysis," NASA Rep. CR-1259, Jan. 1969.

[8] R.C. Dorf, *Time-Domain Analysis and Design of Control Systems.* Reading, Mass.: Addison-Wesley, 1965.

[9] Y. Takahashi, M. Rabins, and D. Auslander, *Control.* Reading, Mass.: Addison-Wesley, 1965.

[10] A.P. Sage, *Optimum Systems Control.* Englewood Cliffs, N.J.: Prentice-Hall, 1968.

[11] A. Fermelia, "Development of helicopter flight path models utilizing modern control techniques," Ph.D. diss., Dep. Mechanical Engineering, Univ. Missouri–Rolla, Rolla, 1975.

[12] ———, "Fundamentals of helicopter stability and control," Vertow Division of Boeing Airplane Co., Rep. R242, Feb. 1961.

[13] A. Fermelia, D. Gyorog, and V. Flanigan, "Helicopter motion–Equation linearization," *IEEE Trans. Aerosp. Electron. Syst.,* this issue, pp. 767-782.

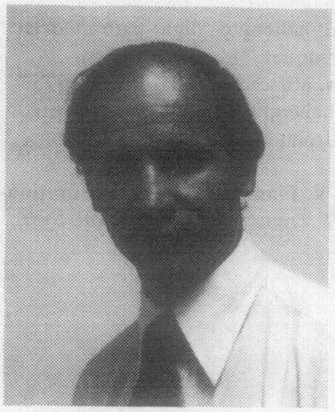

A. Fermelia was born in Rock Springs, Wyo., on April 27, 1942. He received the B.S. degree in mechanical engineering in 1964 from the University of Wyoming, Laramie, the M.S. degree in engineering science in 1966 from the University of California, San Diego, and the Ph.D. degree in 1975 in mechanical engineering from the University of Missouri–Rolla, Rolla.

From 1964 to 1967 he was employed by General Dynamics Convair Division where he was a member of a propulsion group and later a member of the advanced dynamics section. From 1967 to 1970 he was associated with the U.S. Naval Electronics Laboratory Center, San Diego, Calif., where he was concerned with math modeling of a steam generating system and application of estimation theory to the antisubmarine warfare problem. In addition, he has served as a consultant to the U.S. Army Weapons Command, Rock Island, Ill. Currently he is Senior Staff Officer with Hughes Aircraft Company, Aurora, Colo., concerned with math modeling and application of estimation theory to physical systems.

D.A. Gyorog received the B.S. and M.S. degrees in mechanical engineering from the University of Iowa, Iowa City, in 1954 and 1955, respectively, and the Ph.D. degree in mechanical engineering from the University of Wisconsin, Madison, in 1963.

He is currently the Director of Small Arms Directorate, Rodman Laboratory, Rock Island Arsenal, Rock Island, Ill. His engineering experience includes past associations with the U.S. Army Aviation Systems Command, the Air Research Manufacturing Company, the Boeing Corporation, and NASA. In addition, he has held faculty positions as Professor of Mechanical and Aerospace Engineering at the University of Missouri–Rolla and at Arizona State University, Tempe.

Virgil J. Flanigan received the Ph.D. degree in mechanical engineering in 1968 from the University of Missouri–Rolla.

He was appointed as Assistant Professor in mechanical engineering at the University of Missouri–Rolla in 1967 and is now an Associate Professor. He has industrial experience with the Boeing Co. in the Saturn Program, the Western Electric Co. in the wired equipment manufacturing area, and is a consultant to the naval Weapons Center, China Lake, Calif., in the Optics and Guidance Group.

Dr. Flanigan is a member of the American Society of Mechanical Engineers and a registered Professional Engineer in Missouri.